CHEMICAL ENGINEERING TRANSACTIONS
VOL. 70, 2018
A publication of AIDIC
The Italian Association of Chemical Engineering
Online at www.aidic.it/cet
Guest Editors:Timothy G. Walmsley, Petar S. Varbanov, Rongxin Su, Jiří J. Klemeš

ISBN978-88-95608-67-9; **ISSN** 2283-9216
DOI: 10.3303/CET1870040

Bimetallic nZVI-induced Chemical Denitrification Modelling Using the Shrinking Core Model

Giorgio Vilardi

Department of Chemical Engineering Materials Environment, Sapienza University of Rome
giorgio.vilardi@uniroma1.it

In this work the shrinking core model was used for the mathematical modelling of Cu(II)/Fe(0)-induced chemical denitrification in aqueous system. The nano-zero valent iron particles have already been demonstrated their efficiency in the nitrate removal process, and various authors have investigated the influence of several parameters, such as pH and Fe(0)/NO_3^- molar ratio, on the process. In particular, the addition of a second metal, such as Cu, has proved to improve the kinetic of the overall process, allowing to reduce also the nano-particle surface passivation. The present study reports the classical formulation of the shrinking-core model, applying it to the Fe(0)-Cu(II)/NO_3^- aqueous system. The static-film simplified hypothesis was assumed and the electrolyte transport equations for dilute system were considered to take into account in the model the influence of other ion species in solution. The model was then employed to fit the experimental data reported in a previous work, in order to estimate the diffusional and kinetic parameter of the process.

1. Introduction

Nitrate removal from urban wastewater (Stoller et al., 2014) and from contaminated groundwater represented a severe environmental issue (De Filippis et al., 2013) and various technologies, applied also in more complex liquid matrix (Ochando-Pulido et al., 2014) such as membrane processes (Ochando-Pulido and Stoller, 2015), AOPs (De Filippis et al., 2011), photocatalysis (Stoller et al., 2015), or a combination of these processes (Vuppala et al., 2017), have been successfully used to treat organic (Bavasso et al., 2016) and nitrogen-polluted wastewaters (Di Palma et al., 2018). Nitrates, are easily transferred from unsatured zone to the satured one, depending on soil characteristics (Di Palma et al., 2007), as for heavy metals (Di Palma et al., 2011), such as copper (Di Palma, 2009) due to their solubility and low sorptivity on soil particles, caused by their negative charge (De Filippis et al., 2013). The denitrification effectiveness and rapidity strongly depend on the reducing agent, the contact time, the medium characteristics (pH, dissolved oxygen concentration, heavy metals and organic matter concentration) and reactor type (Di Palma et al., 2003) and mixing efficiency (Di Palma and Verdone, 2009).
Nano zero-valent iron particles (nZVI) are characterized by large specific surface area and noticeable chemical activity, able to remove various pollutants in aqueous solutions and contaminated soils, in particular heavy metals such as Cr(VI) (Di Palma et al., 2015) and U (Jing et al., 2016), showing significant removal efficiency in comparison with conventional processes (Marsili et al., 2007), such as the biological one (Marsili et al., 2005). Various nZVI-surface modifications have been reported in literature to increase the reactivity and efficiency of the pollutant removal processes: biopolymers and second metal additions were the most effective attempts to produce more disperse and reactive nano-particles (Vilardi and Di Palma, 2017). nZVI for the nitrate removal in aqueous solutions have already been successfully employed, showing noticeable nitrate conversion to ammonia and nitrogen gas (Suzuki et al., 2012).
Suzuki et al. (2012) proposed two mechanisms for the reduction of nitrates by nZVI:

1. Direct reduction of nitrates ions onto the nZVI surface (the electrons are transferred directly from the Fe(0) core to the adsorbed nitrates ions);
2. Indirect reduction of nitrates ions by hydrogen produced in the liquid bulk after the nZVI acid corrosion.

Please cite this article as: Vilardi G., 2018, Bimetallic nzvi-induced chemical denitrification modelling using the shrinking core model , Chemical Engineering Transactions, 70, 235-240 DOI:10.3303/CET1870040

The major product of nZVI-induced denitrification is ammonia (Suzuki et al., 2012), whereas only a negligible aliquot of nitrates is reduced to nitrogen gas and nitrite, that generally immediately tend to be oxidized again to nitrates (Bavasso et al., 2016).
This work reports about the application of the shrinking core model for the interpretation and modeling of data reported in a previous work (Vilardi and Di Palma, 2017). In particular, the influence of other ions species in the liquid bulk on the nitrate ions transport through the liquid film around the nZVI-Cu particles was taken in consideration. The experimental data were used in a non-linear data fitting procedure for the estimation of kinetic and diffusional constants of the overall transport and chemical reduction process.

2. Shrinking core model and hypothesis

The chemical reaction that occurs in the nZVI-Cu-NO_3^- aqueous system is reported below:

$$3Fe(0) + NO_3^- + H_2O \rightarrow Fe_3O_4 + NH_4^+ + 2OH^- \quad (1)$$

Thus, the iron oxide and ammonia ion are considered the only and final products of nitrate reduction. The following hypotheses were assumed for the model:

1. nZVI nanoparticles are assumed to be spherical and characterized by mean diameter of 78 nm and a radius, r_p, of 36 nm (Vilardi and Di Palma, 2017).
2. The reaction among nitrates and iron nanoparticles occurs onto the nZVI surface after the diffusion of NO_3^- through the liquid film around the particles.
3. The diffusion coefficient D_N^b (m^2/s) of nitrates is influenced by the presence of SO_4^{2-}, Na^+, Cu^{2+}, Cl^-, BO_3^{3-} and K^+ (that are present in the liquid bulk from the dissolution of the iron precursor, reducing agent and target pollutant) according to the following equation (Newman and Thomas-Alyea, 2004):

$$D_N^b = D_N^0 - \frac{t_N}{z_N}\sum_j^3 z_j D_j^0 \frac{Grad(i_j)}{Grad(C_N)} \quad (2)$$

where D^0_N (m^2/s) is the nitrate diffusion coefficient at 25 °C in aqueous solution (Vanysek, 2000), z_N is the valence of nitrate anion, subscript j indicates the other 5 ionic species present in the liquid bulk, i (M) represents the concentration of the j-th ion, C_N (M) is the bulk nitrate concentration, D^0_j (m^2 s^{-1}) is the diffusion coefficient of j-th ion in aqueous solution at 25 °C (Vanysek, 2000), z_j is the valence of the j-th ion and t_N is the chromate transference number, defined as follows(Newman and Thomas-Alyea, 2004):

$$t_N = \frac{C_N D_N^0 z_N^2}{\sum_j^3 z_j^2\, i_j D_j^0} \quad (3)$$

4. There are no temperature or pressure gradient in the reaction medium during the process (perfect mixing conditions).
5. Initially, the iron particles are not porous, and the reaction occurs on their external surface that retracts with the reaction progress with a subsequent oxide shell formation; the reactions occur always at the interface separating the unreacted core from the oxide shell.
6. Nitrate diffusion rate through oxide shell is significantly larger than reaction interface velocity, at the radial distance $r = r_c$ (core radius), thus pseudo-steady-state is considered.
7. Reaction reported in Eq(1) is considered irreversible and of the first-order.
8. During the reactions with nitrates the particle core shrinks uniformly, and at the same time an oxide shell is generated; thus, the particle does not undergo to structural variation during the reaction progress and its dimension remains constant over the time (particle molar density is supposed to be equal to shell molar density).
9. During the reaction progress the nitrate ions are able to diffuse through the oxide shell, characterized by a diffusion coefficient D^m_N.
10. The particles rotational velocity is supposed to be equal to that of liquid, thus a static liquid film is present on the particles (Re = 0). As a consequence, a 'Sherwood number' (Sh) equal to 2 can be fixed and the liquid mass transfer k_L(m/s) can be estimated as follows:

$$k_L = \frac{2D_N^b}{r_p} \quad (4)$$

2.1 Model equations

The dimensionless model equations of Tsakiroglou et al. (2017) were taken in consideration:

$$N_s = \frac{N_b}{1 + {R_c}^2\left(\frac{Da}{Sh}\right) + R_c(1 - R_c)\left(\frac{\delta Da}{\beta}\right)} \tag{5}$$

$$\frac{dR_c}{d\tau} = -\left(\frac{3L^2 m_{Fe} N_b^0 Da}{\rho_{Fe} r_p^2}\right) N_s \tag{6}$$

$$\frac{dN_b}{d\tau} = -\left(\frac{3L^2 m_{Fe} C_{Fe}^0 Da}{\rho_{Fe} r_p^2}\right) N_s {R_c}^2 \tag{7}$$

where NS and NB are the dimensionless nitrate concentrations on the reactive solid core and in the liquid bulk, respectively, $R_c = r_c/r_p$, $Da = kr_p/D^m{}_N$ is the second Damkohler number, k (m/s) is the intrinsic first-order kinetic constant, δ is the tortuosity (assumed equal to 3) and β the porosity of the oxide shell (estimated from the specific surface area reported by Eglal and Ramamurthy (2014) and equal to 0.51), ρ_{Fe} (kg/m^3) is the iron density, m_{Fe} (kg) is the nZVI bimetallic particle mass, $\tau = tD^b{}_N/L^2$, L (m) is the diameter of the reactor vessel used during the experiments, $N^0{}_b$ (M) and $C^0{}_{Fe}$ (M) are the initial bulk concentration of nitrate and the initial nZVI concentration in the reactor.

Finally, the local (X) and global (X_g) particle conversions can be expressed as follows:

$$X = 1 - {R_c}^3 \tag{8}$$

$$X_g = \frac{3}{r_p^3}\int_0^{r_p} r^2 X\, dr \tag{9}$$

The model was then implemented in gPROMS ver.3.4 environment and the kinetic and diffusional parameter values were estimated by non-linear experimental data regression using the optimizer of the same software (Bubbico et al., 2014).

3. Results and discussion

Performance of the shrinking core model was investigated using the experimental data reported by Vilardi and Di Palma (2017) for nitrate removal by Fe/Cu nanoparticles, in aqueous medium: a nitrate solution (0.1 g/L) was tested to investigate the reaction kinetic of nitrate removal using various concentrations of bimetallic nanoparticles (0.05, 0.1, 0.3, 0.5 g/L). Table 1 shows the parameter values adopted for the experimental data regression and kinetic/diffusional parameter optimization (V_s is the volume of liquid in the batch reactor).

Table 1: Model parameter values

Parameter	Unit	Value
L	m	0.052
δ	-	3
ρ_{Fe}	kg/m^3	7860
β	-	0.51
$D^0{}_N$	m^2/s	1.0×10^{-9}
r_p	m	36×10^{-9}
V_s	m^3	2.0×10^{-4}

Figure 1 shows the experimental and model data results, whereas Figure 2 displays the bimetallic nZVI conversion in function of the dimensionless reaction time.

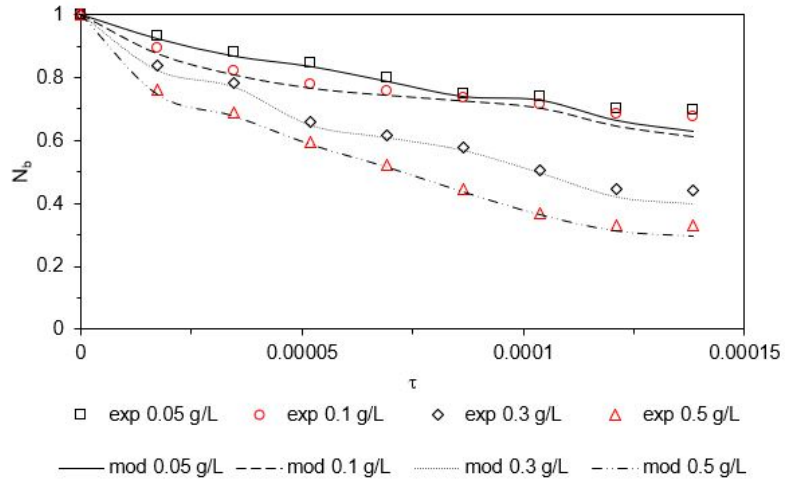

Figure 1: Experimental and modelized nitrate dimensionless bulk concentration over the dimensionless reaction time

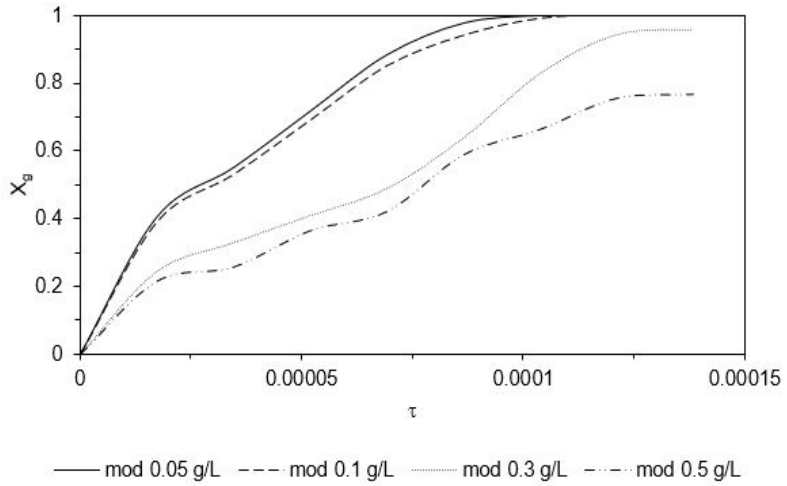

Figure 2: Predicted total bimetallic particles conversion in function of dimensionless reaction time

The model demonstrated to be suitable for the description of the experimental behavior of the reaction Fe(0)/Cu-NO_3^- in aqueous system. Figure 1 displays that the gap among predicted and experimental values is negligible, independently from the bimetallic nanoparticles amount.

On the contrary, the model was not able to well describe the overall bimetallic particle consumption (see Figure 2): in the reaction medium after the 120 min of reaction no active nanoparticles were present. Indeed, considering the reaction reported in Eq(1), a stoichiometric nZVI/NO_3^- molar ratio of 3 can be calculated, implying that the latter two experiments, conducted at C^0_{Fe}= 0.3 and 0.5 g/L, were carried out using an excess of bimetallic nanoparticles, with respect to the stoichiometric request for the theoretical total nitrate conversion. For this reason, the model predicted that an aliquot of nanoparticles was not consumed during the last two experiments.

Actually, besides nitrates, also other three species may react with the nanoparticles, leading to the observed total consumption of the nZVI/Cu at the end of each test: dissolved oxygen, H^+ and water (Vilardi and Di Palma, 2017).

Thus, the Fe(0) was completely consumed even if the total nitrate consumption was never reached. Table 2 reports the optimized kinetic/diffusion parameters and the R^2 values.

Table 2: Kinetic and diffusion optimized parameters

Parameter	nZVI/Cu (g/L) 0.05	nZVI/Cu (g/L) 0.1	nZVI/Cu (g/L) 0.3	nZVI/Cu (g/L) 0.5
k (m/s)	3.40E-04	-	-	-
D^m_N (m^2/s)	4.25E-10	-	-	-
R^2	0.987	0.985	0.993	0.992

The R^2 values were always lower than 0.99, indicating that the model should be modified in order to improve the fitness goodness, introducing also the presence of the other chemical species that contributed to nanoparticles consumption. As regard the optimized regressed parameters values, the following consideration can be drawn:

1. The regressed k value was 2 orders of magnitude lower with respect to the k_L calculated through Eq(4) (about 5.56×10^{-2} m/s). This is in agreement with the assumption that the nitrate diffusion through the liquid film around the nanoparticles was not the limiting step of the overall phenomenon.
2. The regressed D^m_N value was 3 orders of magnitude lower in comparison with the nitrate bulk diffusion coefficient calculated through Eq(2) (about 0.92×10^{-9} m^2/s) and this agrees with the expectations, considering that the diffusion of the same ion through a porous solid particle is always lower than the diffusion in a liquid bulk.
3. The Da value, calculated with the obtained k and D^m_N values was 2.88×10^2, indicating that the nitrates reduction process was characterized by diffusion limits.

4. Conclusions

To describe the overall nitrates/Fe(0)/Cu reaction in aqueous system. the classical shrinking core model was used, considering that only nitrates contributed in the Fe(0) consumption. The model was able to well describe the nitrate reduction by means of nZVI particles until 120 min of reaction time, taking into account both diffusional and chemical mass-transfer phenomena. However, the model was not able to predict the observed total nZVI consumption, because of it did not take into account also the possible corrosion (i.e. metallic iron consumption) due to the presence of other chemical species that may lead to the nanoparticles oxidation (i.e. dissolved oxygen, protons and water). The multiple non-linear regression of the four experimental data sets allowed to obtain the optimized k and D^m_N values, equal to 3.40×10^{-4} m/s and $4.25 \times 10^{-12}$$m^2$/s, respectively; these values were in agreement with the theoretical considerations and assumptions made in this work. Another important result was the obtained Da value of 2.88×10^2 that indicated that the process was characterized by diffusion limits. Therefore, the future work should be addressed to introduce other equations and modifications in the model, in order to develop a more general model, able to predict kinetic and diffusion parameters in a more reliable way, necessary for the process scale-up on a real treatment plant scale.

References

Bavasso I., Di Palma L., Petrucci E., 2016, Treatment of wastewater in H-Type MFC with protonic exchange membrane: experimental study of organic carbon and ammonium reduction with electrochemical characterization, Chem. Eng. Trans., 47, 223–228.

Bubbico R., Mazzarotta B., Verdone N., 2014, CFD analysis of the dispersion of toxic materials in road tunnels, J. Loss. Prev. Process. Ind., 28, 47-59.

De Filippis P., Di Palma L., Scarsella M., Verdone N., 2013, Biological denitrification of high-nitrate wastewaters: A comparison between three electron donors, Chem. Eng. Trans., 32, 319–324.

De Filippis P., Liuzzo G., Scarsella M., Verdone N., 2011, Oxidative desulfurization II: Temperature dependence of organosulfur compounds oxidation, Ind. Eng. Chem. Res., 50, 10452-10457.

Di Palma L., 2009, Influence of indigenous and added iron on copper extraction from soil, J. Hazard. Mater., 170, 96–102.

Di Palma L., Bavasso I., Sarasini F., Tirillò J., Puglia D., Dominici F., Torre L., 2018, Synthesis, characterization and performance evaluation of Fe3O4/PES nano composite membranes for microbial fuel cell, Eur. Polym. J., 99, 222–229.

Di Palma L., Ferrantelli P., Merli C., Petrucci E., Pitzolu I., 2007, Influence of soil organic matter on copper extraction from contaminated soil, Soil Sediment Contam., 16, 323–335.

Di Palma L., Gonzini O., Mecozzi R., 2011, Use of different chelating agents for heavy metal extraction from contaminated harbour sediment, Chem. Ecol., 27, 97–106.

Di Palma L., Gueye M.T., Petrucci E., 2015, Hexavalent chromium reduction in contaminated soil: A comparison between ferrous sulphate and nanoscale zero-valent iron, J. Hazard. Mater., 281, 70–76.

Di Palma, L., Merli, C., Paris, M., Petrucci, E., 2003, A steady-state model for the evaluation of disk rotational speed influence on RBC kinetic: model presentation, Bioresour. Technol., 86, 193–200.

Di Palma L., Verdone N., 2009, The effect of disk rotational speed on oxygen transfer in rotating biological contactors, Bioresour. Technol., 100, 1467–1470.

Eglal M.M., Ramamurthy A.S., 2014, Nanofer ZVI: Morphology, particle characteristics, kinetics, and applications, J. Nanomater., 2014, 1–11.

Jing C., Li Y.L., Landsberger S., 2016, Review of soluble uranium removal by nanoscale zero valent iron, J. Environ. Radioact., 164, 65–72.

Marsili E., Beyenal H., Di Palma L., Merli C., Dohnalkova A., Amonette J.E., Lewandowski Z., 2005, Uranium removal by sulfate reducing biofilms in the presence of carbonates, Water Sci. Technol., 52, 49–55.

Marsili E., Beyenal H., Di Palma L., Merli C., Dohnalkova A., Amonette J.E., Lewandowski Z., 2007, Uranium Immobilization by Sulfate-Reducing Biofilms Grown on Hematite, Dolomite, And Calcite. Environ. Sci. Technol., 41, 8349–8354.

Newman J.S., Thomas-Alyea K.E., 2004, Electrochemical systems. John Wiley and Sons.

Ochando-Pulido J.M., Stoller M., 2015, Kinetics and boundary flux optimization of integrated photocatalysis and ultrafiltration process for two-phase vegetation and olive washing wastewaters treatment, Chem. Eng. J., 279, 387–395.

Ochando-Pulido J.M., Stoller M., Di Palma L., Martinez-Ferez A., 2014, Threshold performance of a spiral-wound reverse osmosis membrane in the treatment of olive mill effluents from two-phase and three-phase extraction processes, Chem. Eng. Process., 83, 64–70.

Stoller M., Pulido J. M. O., Di Palma L., 2014, The relationship between suspended solids of different size, the observed boundary flux and rejection values for membranes treating a civil wastewater stream, Membrane, 4, 414-423.

Stoller M., Ochando-Pulido J.M., Di Palma L., Martinez-Ferez A., 2015, Membrane process enhancement of 2-phase and 3-phase olive mill wastewater treatment plants by photocatalysis with magnetic-core titanium dioxide nanoparticles, J. Ind. Eng. Chem., 30, 147–152.

Suzuki T., Moribe M., Oyama Y., Niinae M., 2012, Mechanism of nitrate reduction by zero-valent iron: Equilibrium and kinetics studies, Chem. Eng. J., 183, 271–277.

Tsakiroglou C.D., Hajdu K., Terzi K., Aggelopoulos C., Theodoropoulou M., 2017, A statistical shrinking core model to estimate the overall dechlorination rate of PCE by an assemblage of zero-valent iron nanoparticles, Chem. Eng. Sci., 167, 191–203.

Vanysek P., 2000, Ionic conductivity and diffusion at infinite dilution. CRC Handbook of Chemistry and Physics, 83.

Vilardi G., Di Palma L., 2017, Kinetic Study of Nitrate Removal from Aqueous Solutions Using Copper-Coated Iron Nanoparticles, Bull. Environ. Contam. Toxicol., 98, 359–365.

Vuppala S., Di Palma L., Cianfrini C., Stoller M., 2017, Flocculation and Nanofiltration Processes with Insight of Fouling Phenomena for the Treatment of Olive Mill Wastewater, Chem. Eng. Trans., 60, 265–270.